NANO LETTERS

2009
Vol. 9, No. 5
1747-1751

Electroluminescence from Suspended and On-Substrate Metallic Single-Walled Carbon Nanotubes

Liming Xie,[†,||] Hootan Farhat,[‡] Hyungbin Son,[†] Jin Zhang,[*,||] Mildred S. Dresselhaus,[§,†] Jing Kong,[*,†] and Zhongfan Liu[||]

Department of Electrical Engineering and Computer Science, Department of Materials Science and Engineering, Department of Physics, Massachusetts Institute of Technology, Cambridge, Massachusetts 02139, and Beijing National Laboratory for Molecular Sciences, College of Chemistry and Molecular Engineering, Peking University, Beijing 100871, People's Republic of China

Received October 3, 2008; Revised Manuscript Received January 17, 2009

ABSTRACT

In this work, we carried out electroluminescence (EL) measurements on metallic single-walled carbon nanotubes (SWNTs) and compared the light emission from the suspended section with the on-substrate section along the same SWNT. In addition to the lowest excitonic emission for metallic SWNTs (M_{11}), a side peak was observed at an energy of 0.17−0.20 eV lower than the M_{11} peak, which is attributed to a phonon-assisted sideband. Interestingly, this side peak was only observed from on-substrate sections but not from suspended sections. This is likely due to the higher electric field used in the EL measurement of on-substrate sections and the asymmetric surroundings for on-substrate SWNT sections. When the drain voltage is increased, either a blue shift or a red shift of the M_{11} emission (up to ±20 meV) was observed in different suspended SWNTs. The red shift can be explained by the temperature-dependence of the M_{11} transition energy, whereas the blue shift is surprising and has never been observed before. Some possible mechanisms for the blue shift are discussed.

With their unique electronic properties and one-dimensional structure, single-walled carbon nanotubes (SWNTs) have potential applications in future nanoelectronics and nanophotonics. Photoluminescence (PL) and electroluminescence (EL) have been intensively investigated to understand the fundamental photophysics in SWNTs.[1−6] In both PL and EL studies, substrates have played an important role in influencing the properties of SWNTs.[2,7−9] Up to now, PL has not been observed from semiconducting SWNTs directly grown on substrates,[2] and suspended semiconducting SWNTs give a much higher PL efficiency[10] than surfactant-wrapped semiconducting SWNTs.[5] On the other hand, EL has been observed from all SWNTs (semiconducting or metallic, suspended or on-substrate).[1,4,11] Thus EL is especially useful to investigate the fundamental photophysics of metallic SWNTs as well as substrate effects. Since the EL properties of different SWNT devices (either suspended or on-substrate) are dramatically different,[1,3,4] comparing the EL spectra from suspended and on-substrate sections from the same SWNT will provide further insight into the fundamental physics of SWNTs.

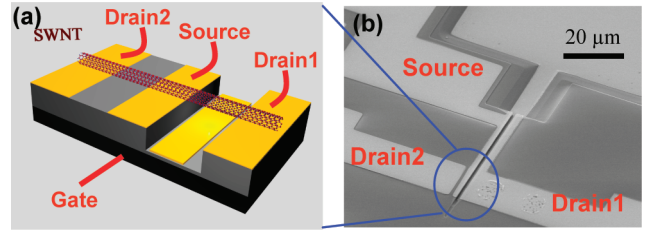

Figure 1. Schematic illustration (a) and scanning electron microscopy image (b) of suspended and on-substrate devices fabricated along the same SWNT.

In the present work, we measured the EL emission from suspended and on-substrate sections along the same metallic SWNT (Figure 1). While the suspended section exhibits a stronger EL signal that turns on at a lower drain voltage V_{ds}, the on-substrate section has an additional side peak at 0.17−0.20 eV below the lowest excitonic transition (M_{11}). This side peak is assigned to phonon-assisted emission. Moreover, in suspended sections, we have observed an interesting blue shift of the EL emission energy at higher

* To whom correspondence should be addressed. E-mail: (J.Z.) jinzhang@pku.edu.cn; (J.K.) jingkong@mit.edu.
[†] Department of Electrical Engineering and Computer Science, Massachusetts Institute of Technology.
[‡] Department of Materials Science and Engineering, Massachusetts Institute of Technology.
[§] Department of Physics, Massachusetts Institute of Technology.
[||] Peking University.

10.1021/nl803004m CCC: $40.75
Published on Web 03/30/2009

drain voltages, which cannot be explained by the temperature dependence of the transition energy M_{11}.

Devices with on-substrate and suspended sections along the same individual SWNTs were fabricated either by transfering[12] or by directly growing ultralong SWNTs by chemical vapor deposition (CVD)[13] onto substrates with prefabricated trenches and electrode patterns. These substrates are the same as those used in ref 11. Briefly, a Si_3N_4 film (thickness $\sim$ 38 nm) was deposited on a SiO_2/Si wafer (oxide thickness = 500 nm). Trenches were then photolithographically defined and etched through the Si_3N_4 on SiO_2. Finally, Pt electrodes (thickness $\sim$ 25 nm) were patterned by lift-off. The CVD growth of ultralong SWNTs was carried out by an Fe-assisted ethanol CVD method.[13] The SWNT transfer was done by a PMMA-mediated transfer method.[12] The EL measurement was achieved by a home-built setup. A 50× aspheric lens was used to collect the EL signal, and a 300 line/mm grating and a 512-pixel InGaAs detector (Hamamatsu G9204−512D, spectrum range 900−1700 nm) were used to disperse the signal and record the spectra. A typical integration time of 60−120 s was used for collecting the spectra. All EL measurements were conducted under an argon atmosphere.

Figure 1a is a schematic illustration of a metallic SWNT device with one section on the Si_3N_4 substrate and the other section suspended. Figure 1b is a scanning electron microscope (SEM) image of a typical device. The highly doped Si substrate was used as a back gate. The channel lengths of the devices are about 1 μm. The trench depth is about 300 nm. Figure 2a shows a typical drain-source current I_{ds} versus drain-source voltage V_{ds} plot of our devices. Due to electron-phonon scattering by optical phonons,[9] for the on-substrate section, I_{ds} saturates at high V_{ds}, and for the suspended section, a negative differential conductance occurs at $V_{ds} >$ 1.2 V. The inset in Figure 2a shows the drain current I_{ds} versus gate voltage (V_{gs}) curve (under constant bias voltage V_{ds} = 10 mV) for the same SWNT (the suspended section), which is a typical $I_{ds}-V_{gs}$ curve for a metallic SWNT. In order to measure EL from individual SWNTs, but not from multiwalled carbon nanotubes or nanotube-bundles, we used the nanotube devices in which the on-substrate sections have saturation currents of about 25 μA.[14,15] The corresponding EL spectra from this SWNT in Figure 2a are presented in Figure 2b. For the suspended section, only one EL peak was observed centered at 1.054 eV at V_{ds} = 2.0 V and V_{gs} = −20 V. Using the diameter information ($\sim$2.3 nm) obtained by atomic force microscopy (AFM) measurements, the 1.054 eV peak from the suspended section can be assigned to the M_{11} excitonic transition.[16] There could be an emission component from the M_{11} continuum that is embedded in the M_{11} exciton emission since the exciton binding energy ($\sim$30 meV for 2.3 nm diameter metallic SWNTs, estimated from the 50 meV reported for a (10,10) SWNT[17]) is less than both the thermal energy (>60 meV[11]) and the EL emission peak width ($\sim$100 meV).

In contrast, for the on-substrate section, two EL peaks (0.865 and 1.036 eV) were observed. Measurements from two other SWNT devices showed similar phenomena,

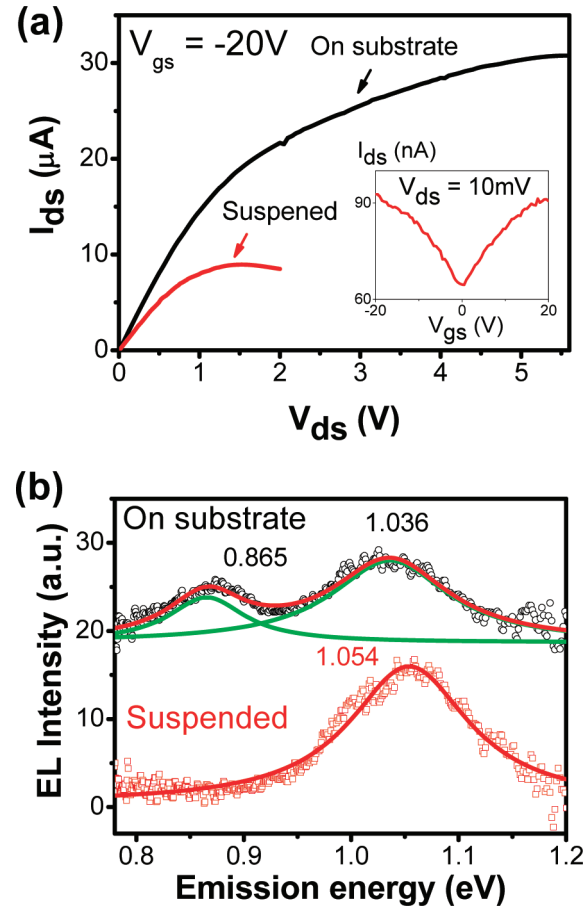

Figure 2. (a) Drain current (I_{ds}) vs drain voltage (V_{ds}) plot for suspended (red line) and on-substrate (black line) sections along the same SWNT. The inset shows the drain current vs gate voltage (V_{gs}) plot for the suspended section. (b) Electroluminescence (EL) from the suspended section (red circle) at V_{ds} = 2.0 V and the on-substrate section (black circle) at V_{ds} = 5.6 V. A gate voltage V_{gs} = −20 V is used in all EL measurements. Data are offset for clarity. Red lines are a Lorentzian fit to the results and green lines are fitting curves for the individual peaks.

namely, the suspended sections only displayed the M_{11} emissions, whereas the on-substrate sections exhibited two emission peaks, one dominant peak near M_{11} of the suspended section and the other one lying 0.17−0.20 eV lower in energy. For the on-substrate sections, a higher V_{ds} is required for observable EL emission. Since the exciton binding energy for a 2.3 nm diameter metallic SWNT is about 30 meV, the two peaks in the emission spectrum of the on-substrate section cannot together be identified as the M_{11} exciton transition and the M_{11} continuum. Additionally, the peak separation does not correspond to the trigonal-warping induced splitting of the M_{11} transition which is less than 70 meV for a 2.3 nm diameter metallic SWNT.[18] Considering that the energy difference between the two peaks ($\sim$0.17 eV) is close to a Γ-point optical phonon energy ($\sim$0.2 eV) and a K-point phonon energy (0.16 eV), the lower energy side peak is assigned to an optical phonon-assisted emission (either from the Γ or K point. From our later discussion, it appears that a Γ-point optical phonon-assisted emission is more likely). Thus the higher energy peak is assigned to the M_{11} emission. Additionally, the M_{11} emission from the on-

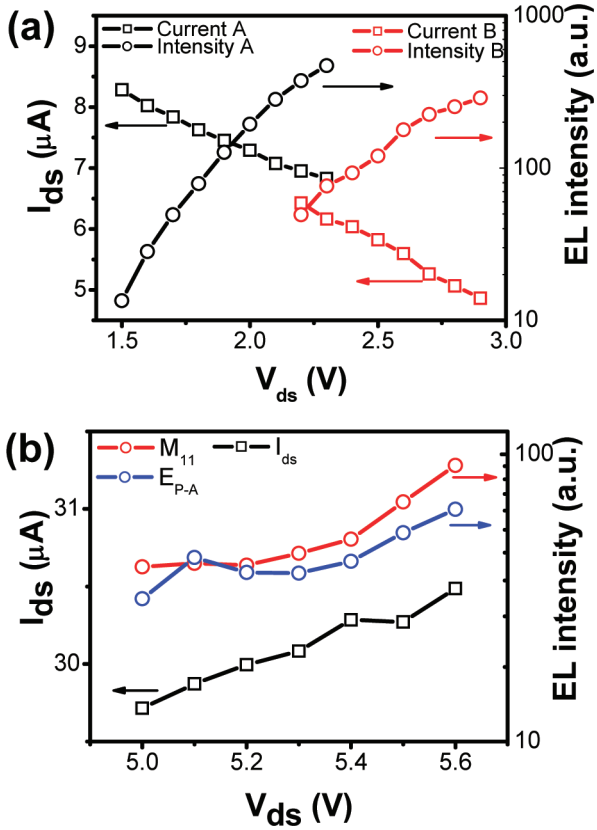

Figure 3. (a) Drain current (I_{ds}) and EL intensity plot vs drain voltage (V_{ds}) for two suspended SWNTs A and B. (b) Drain current (I_{ds}) and EL intensity plot vs drain voltage (V_{ds}) for the same on-substrate section of the SWNT used in Figure 2. M_{11} and E_{P-A} denote the lowest excitonic transition and phonon-assisted emission, respectively.

substrate section was found to be redshifted with respect to the suspended section as will be discussed later.

The drain current and emission intensity versus drain voltage are plotted in Figure 3. For suspended sections, similarly to the observation in ref 11, EL was observed in the negative differential conductance region, where I_{ds} decreases with V_{ds} but the EL intensity increases with V_{ds} (Figure 3a). In contrast to the suspended SWNTs, I_{ds} for the on-substrate SWNT section used in Figure 2 continues to increase with V_{ds} under a large bias of up to 5.6 V, as shown in Figure 3b. But the EL intensity dependence on V_{ds} for the on-substrate section is different from that observed for the suspended sections. The emission intensity for both the phonon-assisted transition (E_{P-A}) and the M_{11} emission for the on-substrate section increased slowly in the range V_{ds} = 5.0−5.4 V and then increased more rapidly in the range V_{ds} = 5.4−5.6 V.

Now we shift our attention to the origin of the phonon-assisted emissions. This phonon-assisted sideband was only observed from the on-substrate sections. Before discussing this difference, the EL mechanisms for suspended and on-substrate SWNTs should be discussed in more detail. Previous works[11,19] have shown that the EL from suspended metallic SWNTs occurs via a thermal light emission mechanism. In this case, hot electrons are thermally distributed in higher energy bands. However, for on-substrate metallic

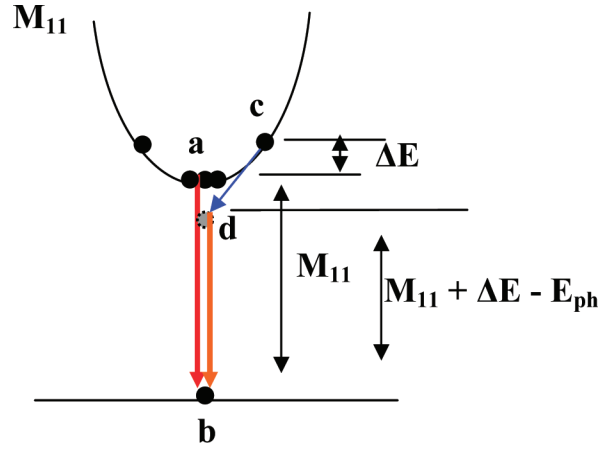

Figure 4. Schematic diagram for direct M_{11} emission (a→b) and phonon-assisted emission (c→d→b). Black dots denote excitons. The phonon-assisted emission energy is $M_{11} + \Delta E - E_{ph}$, where M_{11} is the lowest excitonic transition energy for metallic SWNTs, ΔE is the average energy difference between the excitons at "c" and the excitons at "a", and E_{ph} is the phonon energy.

SWNTs, no EL mechanism has previously been reported. Since suspended SWNTs give observable thermal light emission above 800 K,[11] and on-substrate metallic SWNTs can be heated up to 900 K in air before they burn[20] (in an Ar atmosphere, the same on-substrate SWNT devices can go up to an even higher V_{ds}, indicating that on-substrate SWNTs can go up to a higher temperature), thermal light emission should also be possible for on-substrate metallic SWNTs. Impact excitation, which occurs under a high electrical field,[1,21] is another possible mechanism for EL emission from on-substrate metallic SWNTs. The average electrical field in our EL experiment is about 5 V/μm. The electrical field in the regions of the contacts, defects, and impurities may be higher.

For the energy difference between the sideband and the M_{11} emission, two other SWNTs give an energy difference of 0.20 and 0.17 eV. Since different exciton levels in 1 nm diameter semiconducting SWNTs only have an energy difference of <40 meV[22,23] and the exciton binding energy in metallic SWNTs is much smaller than that in semiconducting SWNTs,[17,24] the energy difference for different exciton levels is much smaller in 2 nm diameter metallic SWNTs. Therefore, the K-point phonon-assisted E symmetry exciton emission should appear at slightly less than 0.16 eV lower energy than the bright exciton emission[23] and the Γ-point phonon-assisted emission should appear at slightly less than 0.20 eV lower than the bright exciton emission. Therefore, the sideband observed in our EL measurement is more likely to be the Γ-point phonon-assisted emission. The smaller observed energy difference (0.17 eV) relative to 0.2 eV is attributed to the kinetic energy of excitons.

Figure 4 depicts the processes of the M_{11} emission (a→b) and the phonon-assisted emission (c→d→b). The intensity of the phonon-assisted emission is related to the number of excitons distributed above the M_{11} band edge with nonzero momentum and the efficiency for these excitons to emit via the phonon-assisted process. For the on-substrate sections, there may be more higher-energy excitons with nonzero

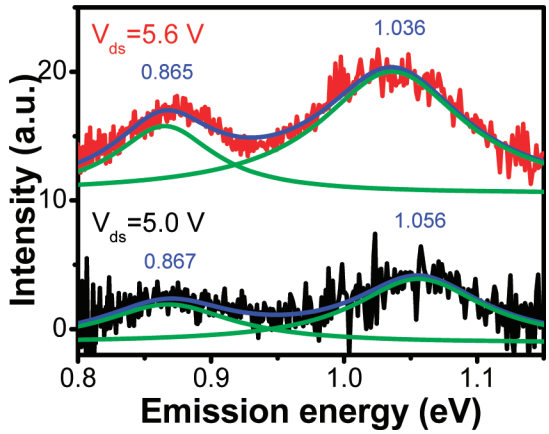

Figure 5. EL from the on-substrate section of the SWNT used in Figure 2 at different drain voltages. Red line for $V_{ds} = 5.6$ V, black line for $V_{ds} = 5.0$ V. (For both data sets V_{gs} is at -20 V.) Blue lines are a Lorentzian fit to the emissions and green lines are fitting curves for the individual peaks.

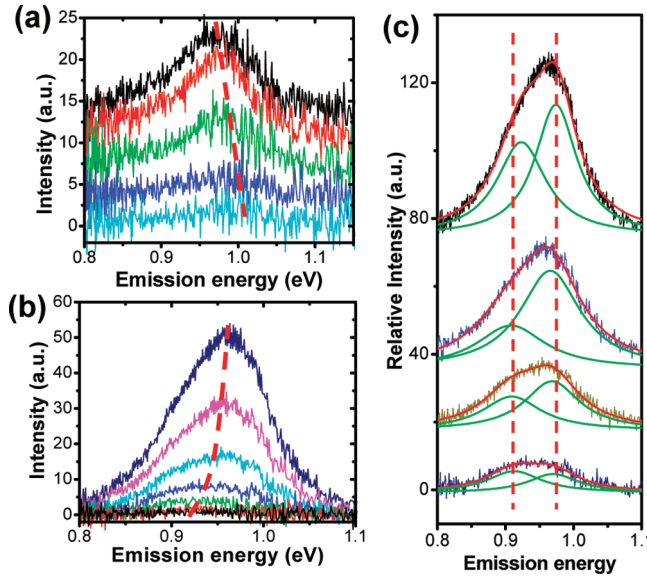

Figure 6. Red shift (a) and blue shift (b) of the EL emission position with increasing drain voltage observed for suspended sections of two different metallic SWNTs. The dashed red lines are guidance for the eyes. From bottom to top in panel a, $V_{ds} = 2.0-2.4$ V with steps of 0.1 V; in panel b, $V_{ds} = 1.0-1.6$ V with steps of 0.1 V. For all data sets V_{gs} is at -20 V. (c) A two-Lorentzian peak fit to the emission profiles from the suspended SWNT in panel b; from bottom to up, $V_{ds} = 1.3-1.6$ V with a step of 0.1 V.

momentum because a higher electric field was used in the EL measurements of the on-substrate sections, and this higher electric field will accelerate the carriers more and may create more excitons with higher energy and nonzero momentum.[21] Meanwhile, the suspended metallic SWNTs may have a very low phonon-assisted emission efficiency judging from PL studies of semiconducting SWNTs. Up to now there has been no report of phonon-assisted PL from suspended semiconducting SWNTs. But phonon-assisted PL emission has been reported from surfactant-wrapped or DNA-wrapped semiconducting SWNTs.[25,26] It is possible that due to their symmetric and unperturbed surroundings, suspended semiconducting SWNTs have a low phonon-assisted efficiency. This may be the same case for our suspended metallic SWNTs, which will account for the absence of phonon-assisted EL emission.

The phonon-assisted emission energy $E_{P\text{-}A}$ can be expressed as $M_{11} + \Delta E - E_{ph}$, where ΔE is the average exciton energy relative to the zero-momentum exciton at the M_{11} edge and E_{ph} is the phonon energy. Because of the nonzero value of ΔE, the energy difference between $E_{P\text{-}A}$ and M_{11} should be less than E_{ph}, which is consistent with the experimental data. At a lower V_{ds}, ΔE is expected to be smaller since in this case there are fewer high-energy excitons in the system. Therefore the energy difference between $E_{P\text{-}A}$ and M_{11} is expected to be larger at lower V_{ds}. This is confirmed by our observations (Figure 5). At $V_{ds} = 5.0$ V, the energy difference between the $E_{P\text{-}A}$ and the M_{11} emission is 0.19 eV. When V_{ds} is changed to 5.6 V, it can be seen that the M_{11} emission is redshifted by 20 meV and the difference between the two peaks becomes 0.17 eV. The red shift of the M_{11} emission could be due to the increase of the lattice temperature at higher V_{ds}.[20]

The energy difference between the M_{11} emissions from the suspended and the on-substrate sections, as shown in Figure 2b, can be attributed to environmental effects (differences in the dielectric constant of the SWNT surroundings, substrate interaction, etc.), dark-bright exciton mixing and/or the temperature difference between the suspended and the on-substrate sections under the EL experimental conditions. Because the dielectric constant of Si_3N_4 ($\varepsilon = 7.5$) is significantly larger than that of air ($\varepsilon = 1$) and the transition energy of SWNTs is smaller in higher dielectric constant surroundings,[7,27] substrates can induce a red shift of M_{11}. Van der Waals interactions with the substrates can induce an elastic deformation in the SWNTs[28] and make their transition energies shift (tens of meV).[29] The asymmetric surrounding and higher electric field required for the emission can introduce a perturbation to the on-substrate sections. Such perturbations can promote dark-bright exciton mixing and also can induce a red shift of the transition energy (by several meV).[30,31] The temperatures for the suspended and on-substrate sections are unknown and the temperature difference may contribute up to a -10 meV shift in the M_{11} transition per 100 K temperature increase.[32]

For the suspended sections, some SWNTs show a red shift and others show a blue shift of the EL peak starting from the V_{ds} at the onset of the EL emission and going to the V_{ds} point just before the SWNTs are burnt out (Figure 6a,b). All EL emission from suspended sections was measured in the negative differential conductance region. Different SWNTs give different maximum energy shifts (between ± 20 meV). For the suspended SWNTs, the lattice temperature of the SWNTs increases with increasing V_{ds}[11] and the transition energies (such as M_{11}) decrease with increasing temperature.[32] Therefore, in some suspended SWNTs the temperature dependence of the transition energies may dominate the EL emission shift, which gives a red shift of the EL emission with increasing V_{ds}. In other SWNTs, other factors may dominate the EL emission shift. Noticing that the EL emission peaks from the suspended section are

asymmetric, the emission profile can be fit by two components: a low-energy component and a high-energy component (Figure 6c). As V_{ds} increases, the intensity of both the low-energy component and the high-energy component increase but the energy of the peak positions of these two components vary only slightly compared to the shift (Figure 6c). However the intensity ratio for the high-energy component to the low-energy component increases with V_{ds} (from 1.3 V to 1.5 V), which gives rise to a blue shift of the overall spectrum. Therefore, this blue shift is due to the relatively higher intensity of the high-energy component. Since suspended SWNTs have a higher temperature at a higher V_{ds},[11] the relatively higher intensity of the high-energy component may correspond to relatively more thermally excited excitons occupying the higher energy level. The higher energy level could be identified as either the M_{11} continuum and/or the M_{11}^+ exciton level (the upper component of the trigonal warping-split M_{11} transition). For the SWNT shown in Figure 6c, the M_{11}^+ exciton emission is the most likely explanation judging from the energy difference between these two emission components (~50 meV).

In conclusion, we have carried out EL measurements on suspended and on-substrate sections of the same metallic SWNTs. A phonon-assisted emission was found from the on-substrate sections, which may be due to the higher electric field and the asymmetric surroundings for the on-substrate SWNT sections. In the suspended SWNT sections, some SWNTs showed a red shift and others showed a blue shift of the EL peak position with increasing V_{ds}. The blue shift, which cannot be understood by a temperature-dependent transition energy, could be caused by the fine features of the emission spectrum at a higher temperature, either by emission from the M_{11} continuum and/or from the upper component M_{11}^+ of the trigonal warping-split transition energies.

Acknowledgment. This work was partially supported by the Materials, Structure, and Device Center, one of the five centers of the Focus Center Research Program (FCRP) and NSF/DMR 07-04197. The authors acknowledge Mr. Xinran Wang, Professor Hongjie Dai, Professor Tony Heinz, Professor Riichiro Saito, and Dr. Georgy Samsonidze for helpful discussions, and Dr. Qian Wang and Professor Hongjie Dai for providing substrates with prepatterned electrodes. L.X. acknowledges a Scholarship from the China Scholarship Council, the Peking University CDY Scholarship. J.K. and J.Z. acknowledges NSFC 20828004.

References

(1) Chen, J.; Perebeinos, V.; Freitag, M.; Tsang, J.; Fu, Q.; Liu, J.; Avouris, P. *Science* **2005**, *310* (5751), 1171–1174.
(2) Lefebvre, J.; Homma, Y.; Finnie, P. *Phys. Rev. Lett.* **2003**, *90* (21), 217401.
(3) Marty, L.; Adam, E.; Albert, L.; Doyon, R.; Menard, D.; Martel, R. *Phys. Rev. Lett.* **2006**, *96* (13), 136803.
(4) Misewich, J. A.; Martel, R.; Avouris, P.; Tsang, J. C.; Heinze, S.; Tersoff, J. *Science* **2003**, *300* (5620), 783–786.
(5) O'Connell, M. J.; Bachilo, S. M.; Huffman, C. B.; Moore, V. C.; Strano, M. S.; Haroz, E. H.; Rialon, K. L.; Boul, P. J.; Noon, W. H.; Kittrell, C.; Ma, J. P.; Hauge, R. H.; Weisman, R. B.; Smalley, R. E. *Science* **2002**, *297* (5581), 593–596.
(6) Xie, L. M.; Liu, C.; Zhang, J.; Zhang, Y. Y.; Jiao, L. Y.; Jiang, L.; Dai, L.; Liu, Z. F. *J. Am. Chem. Soc.* **2007**, *129* (41), 12382–12383.
(7) Walsh, A. G.; Vamivakas, A. N.; Yin, Y.; Cronin, S. B.; Unlu, M. S.; Goldberg, B. B.; Swan, A. K. *Nano Lett.* **2007**, *7* (6), 1485–1488.
(8) Pop, E.; Mann, D.; Cao, J.; Wang, Q.; Goodson, K.; Dai, H. J. *Phys. Rev. Lett.* **2005**, *95* (15), 155505.
(9) Yao, Z.; Kane, C. L.; Dekker, C. *Phys. Rev. Lett.* **2000**, *84* (13), 2941–2944.
(10) Lefebvre, J.; Austing, D. G.; Bond, J.; Finnie, P. *Nano Lett.* **2006**, *6* (8), 1603–1608.
(11) Mann, D.; Kato, Y. K.; Kinkhabwala, A.; Pop, E.; Cao, J.; Wang, X. R.; Zhang, L.; Wang, Q.; Guo, J.; Dai, H. J. *Nat. Nanotechnol.* **2007**, *2* (1), 33–38.
(12) Jiao, L.; Fan, B.; Xian, X.; Wu, Z.; Zhang, J.; Liu, Z. *J. Am. Chem. Soc.* **2008**, *130* (38), 12612–12613.
(13) Zheng, L. X.; O'Connell, M. J.; Doorn, S. K.; Liao, X. Z.; Zhao, Y. H.; Akhadov, E. A.; Hoffbauer, M. A.; Roop, B. J.; Jia, Q. X.; Dye, R. C.; Peterson, D. E.; Huang, S. M.; Liu, J.; Zhu, Y. T. *Nat. Mater.* **2004**, *3* (10), 673–676.
(14) Collins, P. C.; Arnold, M. S.; Avouris, P. *Science* **2001**, *292* (5517), 706–709.
(15) Javey, A.; Guo, J.; Paulsson, M.; Wang, Q.; Mann, D.; Lundstrom, M.; Dai, H. J. *Phys. Rev. Lett.* **2004**, *92* (10), 106804.
(16) Strano, M. S. *J. Am. Chem. Soc.* **2003**, *125* (51), 16148–16153.
(17) Deslippe, J.; Spataru, C. D.; Prendergast, D.; Louie, S. G. *Nano Lett.* **2007**, *7* (6), 1626–1630.
(18) Saito, R.; Dresselhaus, G.; Dresselhaus, M. S. *Phys. Rev. B* **2000**, *61* (4), 2981–2990.
(19) Wang, X.; Zhang, L.; Lu, Y.; Dai, H.; Kato, Y. K.; Pop, E. *Appl. Phys. Lett.* **2007**, *91* (26), 261102.
(20) Pop, E.; Mann, D. A.; Goodson, K. E.; Dai, H. J. *J. Appl. Phys.* **2007**, *101* (9), 093710.
(21) Perebeinos, V.; Avouris, P. *Phys. Rev. B* **2006**, *74* (12), 121410.
(22) Srivastava, A.; Htoon, H.; Klimov, V. I.; Kono, J. *Phys. Rev. Lett.* **2008**, *101* (8), 087402.
(23) Torrens, O. N.; Zheng, M.; Kikkawa, J. M. *Phys. Rev. Lett.* **2008**, *101* (15), 157401.
(24) Wang, F.; Dukovic, G.; Brus, L. E.; Heinz, T. F. *Science* **2005**, *308* (5723), 838–841.
(25) Lebedkin, S.; Hennrich, F.; Kiowski, O.; Kappes, M. M. *Phys. Rev. B* **2008**, *77* (16), 165429.
(26) Chou, S. G.; Plentz, F.; Jiang, J.; Saito, R.; Nezich, D.; Ribeiro, H. B.; Jorio, A.; Pimenta, M. A.; Samsonidze, G. G.; Santos, A. P.; Zheng, M.; Onoa, G. B.; Semke, E. D.; Dresselhaus, G.; Dresselhaus, M. S. *Phys. Rev. Lett.* **2005**, *94* (12), 127402.
(27) Miyauchi, Y.; Saito, R.; Sato, K.; Ohno, Y.; Iwasaki, S.; Mizutani, T.; Jiang, J.; Maruyama, S. *Chem. Phys. Lett.* **2007**, *442* (4−6), 394–399.
(28) Hertel, T.; Walkup, R. E.; Avouris, P. *Phys. Rev. B* **1998**, *58* (20), 13870–13873.
(29) Shan, B.; Lakatos, G. W.; Peng, S.; Cho, K. J. *Appl. Phys. Lett.* **2005**, *87* (17), 173109.
(30) Shaver, J.; Kono, J.; Portugall, O.; Krstic, V.; Rikken, G. L. J. A.; Miyauchi, Y.; Maruyama, S.; Perebeinos, V. *Nano Lett.* **2007**, *7* (7), 1851–1855.
(31) Mortimer, I. B.; Nicholas, R. J. *Phys. Rev. Lett.* **2007**, *98* (2), 027404.
(32) Cronin, S. B.; Yin, Y.; Walsh, A.; Capaz, R. B.; Stolyarov, A.; Tangney, P.; Cohen, M. L.; Louie, S. G.; Swan, A. K.; Unlu, M. S.; Goldberg, B. B.; Tinkham, M. *Phys. Rev. Lett.* **2006**, *96* (12), 127403.

NL803004M